Near-Fastest Battery Balancing by Cell/Module Reconfiguration

Weiji Han, *Student Member, IEEE*, Changfu Zou, *Member, IEEE*, Liang Zhang, *Member, IEEE*, Quan Ouyang, and Torsten Wik

***Abstract*—Charge imbalance is a very common issue in multi-cell/module/pack battery systems due to manufacturing variations, inconsistent charging/discharging, and uneven thermal distribution. As a consequence, the deliverable charge capacity, battery lifespan, and system reliability may all decrease over time. To tackle this issue, various external circuit designs can be attached for charge balance, and the internal battery cell/module/pack connection can also significantly affect the charge balance performance. This paper focuses on minimizing the battery charge equalization (BCE) time by battery cell/module reconfiguration. Specifically, for the reconfigurable module-based BCE system, we propose reconfiguration algorithms for fast charge equalization under different levels of system reconfigurability. For battery systems allowing module reconfiguration and intra-module cell reconfiguration, the proposed module-based bounded reconfiguration algorithm can reach or get very close to the minimum BCE times obtained by exhaustive search. When the reconfigurability level is extended by allowing inter-module cell reconfiguration, the proposed module-based complete reconfiguration algorithm can achieve similar optimality to that of the genetic algorithm (GA). Moreover, as compared to the circuit experiments, exhaustive search, and GA, the proposed algorithms take much less computational time. The optimality and computational efficiency of the proposed algorithms are demonstrated by both circuit and numerical experiments.**

***Index Terms*—Battery system, battery cell/module reconfiguration, battery charge balance/equalization, optimality, computational efficiency.**

I. Introduction

BATTERY systems have been playing very important roles in a variety of applications from small devices such as smartphones and laptop computers to large-scale systems such as electric vehicles [1] and battery energy storage systems in the power grid [2], [3]. In all battery systems including multiple cells/modules/packs, one very common issue affecting system performance is charge imbalance. Battery charge imbalance always exists with repeated charging/discharging because of manufacturing variations in charge capacity, internal impedance, self-discharging rate, inconsistent charging/discharging current, and uneven thermal distribution, etc. [4]–[6]. As a consequence of charge imbalance among battery cells/modules/packs, the system performance deteriorates in terms of early termination of charging/discharging, increased energy loss, accelerated battery degradation, and even safety hazards, such as fire or explosion [6]–[9]. To alleviate battery charge imbalance, two options are typically considered: (1) assigning larger charging (discharging) current to the batteries with lower (higher) charge, and (2) transferring charge from higher-charge batteries to lower-charge ones.

For the first option based on current assignment for charge balance, reconfigurable battery systems are emerging as a promising solution since the connection topology of battery cells/modules/packs can be flexibly and adaptively reconfigured according to real-time system states and charging/discharging requirements [10]–[12]. As summarized in [10], in most reconfigurable battery system designs reported so far, 2 to 6 controllable switches are usually connected to each battery cell and then flexible battery reconfiguration becomes achievable by controlling the switch operations [11]–[15]. A few recent studies investigated how to improve battery charge balance by battery cell/module/pack reconfiguration. For that purpose, a reconfigurable and modular architecture was proposed to facilitate the operation of battery packs under unbalanced conditions in [3]. Battery pack reconfiguration was studied to mitigate battery charge imbalance for increased acceptable (deliverable) charge capacity during charging (discharging) in [16] ([17]). A reconfigurable battery management system was designed in [18] to alleviate charge imbalance by disconnecting the fully charged (discharged) cell during charging (discharging).

To apply the second option to battery charge balance, i.e., by charge transfer, a number of circuit designs and control strategies have been proposed in recent decades [6], [8], [9], [19], [20]. Among these designs, *cell-to-cell charge equalizers* are widely used to balance the charge of two adjacent cells. Based on such charge equalizers, different battery charge equalization (BCE) structures can be developed, such as series-based and module-based BCE structures.

Manuscript received August 19, 2018; revised March 1, 2019; accepted April 16, 2019. Date of publication May 6, 2019; date of current version October 30, 2019. This work was supported in part by the University of Connecticut and Chalmers University of Technology, and in part by the Swedish Energy Agency under Project 44401-1. Paper no. TSG-01218-2018. *(Corresponding author: Changfu Zou.)*

W. Han, C. Zou, and T. Wik are with the Department of Electrical Engineering, Chalmers University of Technology, 41296 Gothenburg, Sweden (e-mail: weiji.han@chalmers.se; changfu.zou@chalmers.se; tw@chalmers.se).

L. Zhang is with the Department of Electrical and Computer Engineering, University of Connecticut, Storrs, CT 06269 USA (e-mail: liang.zhang@uconn.edu).

Q. Ouyang is with the College of Automation Engineering, Nanjing University of Aeronautics and Astronautics, Nanjing 210016, China (e-mail: ouyangquan@nuaa.edu.cn).

Color versions of one or more of the figures in this paper are available online at http://ieeexplore.ieee.org.

Digital Object Identifier 10.1109/TSG.2019.2915013

Clearly, if the above two options can be combined, i.e., both battery reconfiguration and charge transfer can be performed, the charge balance performance could be further improved and even optimized. This will be the topic investigated in this paper, i.e., how to expedite the charge balance in *reconfigurable module-based battery charge equalization (BCE) systems*, which consists of a series of reconfigurable battery cells with a module-based BCE structure mounted on them (more details about such system will be introduced in Section II).

To evaluate the charge balance performance, one critical measure is the *battery charge equalization (BCE) time*. Not only does the BCE time indicate the duration of battery charge equalization process, but it is also closely related to the total energy loss [21]. For series-connected battery cells, the external charging/discharging current passing through each cell is identical to each other. Then, during the discharging process, the deliverable charge capacity is obviously restricted by the weakest cell (i.e., the cell with the lowest charge). The shorter the BCE time, the sooner all charge in the system becomes available to be delivered (i.e., all cells can be fully discharged). Similarly, for the charging process of series-connected battery cells, only after all cells reach charge equalization can all charging space in the system be completely utilized (i.e., all cells can be fully charged). The BCE time of a battery system depends on both the BCE structure applied and the configuration of all battery cells/modules/packs. Given the same BCE structure, the battery configuration can significantly affect the BCE time. For example, for a module-based BCE system including 3 modules and 2 cells per module with initial cell SOCs ranging from 0.72 to 0.8, the BCE time was found to vary by almost a factor 2 with different battery cell/module configurations based on the simulation results in [22]. Motivated by this, we aim to search the battery cell/module configuration leading to the fastest charge equalization, i.e., minimizing the BCE time by battery reconfiguration.

To optimize the battery cell/module configuration for fast charge equalization, the first constraint we have to consider is the reconfigurability level of battery systems. In a large-scale battery system, battery cells are typically grouped into a number of modules, and then the modules are further grouped into packs. For example, in the world's largest lithium-ion battery storage facility, 400,000 battery cells are installed in nearly 20,000 modules, and placed in 24 containers/packs [23]. For such large-scale systems, the reconfiguration could be performed on cell, module, or pack levels. Depending on the reconfigurability of the battery system, possible cell/module/pack configurations can be described by certain permutations, and the total number can thus easily reach a vastly large number. For instance, for a battery system with 20 reconfigurable cells connected in series, the total number of cell configurations can reach $20! \approx 2.433 \times 10^{18}$. Clearly, even for moderately sized systems, it already becomes infeasible to achieve the optimal battery cell/module/pack configuration by an exhaustive search. Therefore, in this paper we will develop battery reconfiguration algorithms to identify the battery cell/module configurations leading to the fastest or near-fastest charge equalization under different levels of reconfigurability in module-based BCE systems. As the major contribution of this paper, these proposed algorithms are developed through a series of in-depth analysis of the BCE time calculation formulas along with some necessary local searches, and thus demonstrate very high computational efficiency while maintaining the optimality.

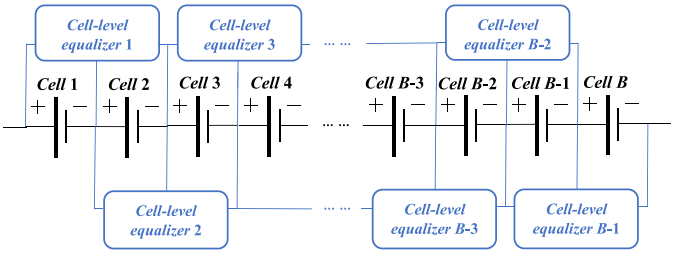

Fig. 1. Cell-level series-based BCE system.

The remainder of this paper is organized as follows. In Section II, the module-based BCE system and the formulas to calculate its BCE time are introduced. For such systems, the practical circuit designs for battery reconfiguration are reviewed and the mathematical models for the optimal battery cell/module configurations under different levels of reconfigurability are discussed in Section III. Then, the optimal module configuration and intra-module cell configurations are studied in Section IV. The study is extended in Section V by considering the cell reconfiguration across battery modules, and the optimality and computational efficiency of the proposed algorithm are compared with the results obtained from the genetic algorithm. Finally, conclusions and future work are presented in Section VI.

II. Module-Based BCE System

A. System Modeling

A variety of circuit designs have been proposed to perform battery charge balancing/equalization [24]. These circuit designs could significantly differ from each other, which makes it difficult to develop some universal models and methods applicable to all. Thus, we base our research on a class of widely used battery equalizers, i.e., cell-to-cell battery equalizers.

Series-connected battery systems are typically used in practical applications to provide high total voltage. To balance the charge among series-connected battery cells, electrical devices called *cell-level charge equalizers* can be connected to each pair of consecutively connected cells (see Fig. 1 for illustration). Such a system is referred to as a *cell-level series-based battery charge equalization (BCE) system* [25].

Based on the series-based BCE system, the module-based BCE system can be designed as follows. Consider a battery system consisting of M modules connected in series, as shown in Fig. 2. In order to balance the charge of these M modules, $M-1$ *module-level charge equalizers* are connected to every two adjacent modules. Accordingly, this system is referred to as a *module-level series-based BCE system*. In addition, if each module in the system is a cell-level series-based BCE system,

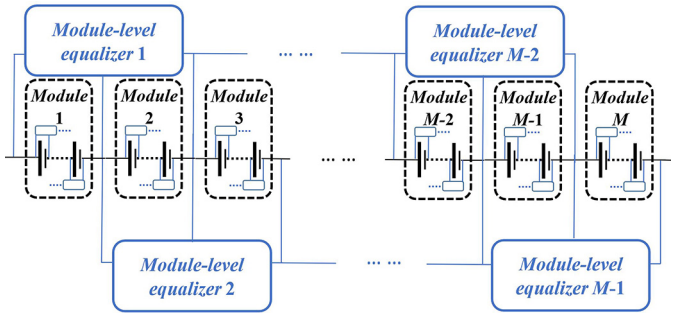

Fig. 2. Module-based BCE system.

we refer to the entire system as a *module-based BCE system*. Thus, in a module-based BCE system including M modules as shown in Fig. 2, there exists a total of $M+1$ subsystems: one module-level and M cell-level series-based BCE subsystems. As compared to the series-based BCE system, the module-based BCE system features improved system performance, such as faster charge equalization, due to the introduction of module-level battery charge equalizers. Besides, since the module-based BCE system could be reconfigured on both cell and module levels, more flexible battery reconfiguration can be enabled to boost the system performance.

In the module-based BCE system, to facilitate the system control, it is assumed that the working cycles of all module-level and cell-level charge equalizers are synchronized with the same duration, denoted by τ. Each battery cell's state is described by its state of charge (SOC), which is defined by the ratio of the cell's current amount of charge and its rated charge capacity denoted by C_B. Then, in a module-based BCE system with M modules and B cells per module, the i-th cell's SOC at time instant t is denoted by $x_i(t)$, $i = 1, 2, \ldots, M \times B$.

At the beginning of a working cycle, each cell-level charge equalizer compares the charge of the two cells connected to it. Then during the working cycle, the cell-level equalizer extracts $r_c C_B$ amount of charge from the cell with higher charge and transfers $(1-l_c)r_c C_B$ amount of charge to the cell with lower charge, while $l_c r_c C_B$ amount of charge is lost during the transfer (e.g., to be dissipated as heat). Here, r_c and l_c denote the cell-level charge transfer rate and cell-level charge transfer loss rate, respectively. Note that, since the charge transfer direction of each equalizer remains unchanged throughout each working cycle, battery SOCs rarely reach exact equalization when the transfer direction is updated at the beginning of next working cycle (some discrete time instants on the time axis). As a result, when only some battery SOCs are approaching equalization, they usually demonstrate zigzag evolution as given in [26], which still triggers the charge transfer between cells. When all cell SOCs approach charge equalization, all charge equalizers are forced to stop working and the charge equalization process is terminated. The module-level charge equalizers work in the same manner except that the charge is transferred between every two adjacent battery modules with module-level charge transfer rate r_m and module-level charge transfer loss rate l_m. These assumptions of constant charge transfer rates and loss rates are made for a class of widely used battery charge equalizers with the following property: given various battery cells/modules connected, the charge transfer rate and loss rate are almost constant or only slightly vary within a very narrow range. A typical example is the inductor-based charge equalizer which will be applied in the circuit experiments in Section IV-B. Thus, for such class of battery charge equalizers, the charge transfer rates and loss rates are typically specified by the average rates collected from a group of preliminary circuit experiments.

Note that, as shown in Fig. 2, in a module-based BCE system, since each cell-level BCE subsystem only operates within its own module, the cell-level charge equalization within each individual module is independent of each other. In addition, due to the cell-level charge equalization, during each working cycle the total loss of cell SOCs in each module is identical, i.e., $(B-1)l_c r_c$. Then, the cell-level charge equalization does not change the total cell SOC difference between modules, and thus does not influence the module-level charge equalization. Moreover, since the cells are connected in series in each module, the module-level charge equalization always causes identical SOC change for all cells within the module. In other words, the module-level charge equalization does not affect the cell-level charge equalization either. Therefore, in a module-based BCE system with M modules, all cell-level and module-level charge equalization processes in the $M+1$ subsystems can be regarded as independent operations.

B. Battery Charge Equalization Time

For a module-based BCE system, one important performance measure is the battery charge equalization (BCE) time, which is defined by the time needed for all battery cells to reach charge equalization from their initial states, i.e., the duration of the battery charge equalization process. The BCE time indicates the efficiency of the charge equalization mechanism applied to a battery system. In addition, the BCE time is closely related to other important system performance measures, such as the total energy loss during battery charge equalization. Thus, it is of great importance to assess the BCE time.

As mentioned above, since a module-based BCE system with M modules can be viewed as $M+1$ independently operating series-based BCE subsystems, its BCE time must be the longest one of all $M+1$ subsystems' BCE times. Formulas to calculate the BCE time of a series-based BCE system were derived in our previous work [26]. Based on this idea and [26], the BCE time calculation formulas for module-based BCE systems were derived in another paper [22]. Thus, in this paper, instead of repeating these details, we briefly introduce the general idea with major mathematical notations and only present the final result which can be directly used for calculating the BCE time of module-based BCE systems.

First, for the m-th cell-level series-based BCE subsystem, its BCE time, denoted by $T_e^{cel}(m)$, $m \in \{1, 2, \ldots, M\}$, can be calculated based on [26] as

$$T_e^{cel}(m) = \max_{g \in \{1,\ldots,B-1\}} t^{cel}(m, g), \tag{1}$$

where

$$t^{cel}(m,g)=\begin{cases}\frac{(\bar{x}_{m,g}(0)-\bar{x}_{m,B}(0))\tau}{\left(\frac{1-l_C}{g}+\frac{l_C}{B}\right)r_c}, & \text{if } \bar{x}_{m,g}(0)\geq\bar{x}_{m,B}(0),\\ \frac{(\bar{x}_{m,B}(0)-\bar{x}_{m,g}(0))\tau}{\left(\frac{1}{g}-\frac{l_C}{B}\right)r_c}, & \text{if } \bar{x}_{m,g}(0)<\bar{x}_{m,B}(0),\end{cases}$$

$$\bar{x}_{m,g}(0)=\frac{1}{g}\sum_{i=(m-1)B+1}^{(m-1)B+g}x_i(0),\ g\in\{1,\ldots,B\}.$$

In the above equation, g is the size of the battery group $BG(m,g)$ including the first cell to the g-th cell in the m-th battery module, $\bar{x}_{m,g}(0)$ is the average initial cell SOC of $BG(m,g)$, and $t^{cel}(m,g)$ is the shortest time needed for $BG(m,g)$'s average cell SOC to reach the m-th module's average cell SOC.

Then, for the module-level series-based BCE subsystem, each module can be viewed as an "aggregated cell", and thus, the module-level BCE time, denoted by T_e^{mod}, is calculated by

$$T_e^{mod}=\max_{g\in\{1,\ldots,M-1\}}t^{mod}(g), \tag{2}$$

where

$$t^{mod}(g)=\begin{cases}\frac{(\overline{X}_g(0)-\overline{X}_M(0))\tau}{\left(\frac{1-l_m}{g}+\frac{l_m}{M}\right)r_m}, & \text{if } \overline{X}_g(0)\geq\overline{X}_M(0),\\ \frac{(\overline{X}_M(0)-\overline{X}_g(0))\tau}{\left(\frac{1}{g}-\frac{l_m}{M}\right)r_m}, & \text{if } \overline{X}_g(0)<\overline{X}_M(0),\end{cases}$$

$$\overline{X}_g(0)=\frac{1}{g}\sum_{m=1}^{g}X_m(0),\quad g\in\{1,\ldots,M\},$$

$$X_m(t)=\sum_{i=(m-1)B+1}^{mB}x_i(t),\quad m\in\{1,2,\ldots,M\},\ t\geq 0.$$

Finally, let T_e^{sys} denote the BCE time of the module-based BCE system and it is given by

$$T_e^{sys}=\max\left\{T_e^{cel}(1),\ldots,T_e^{cel}(M),T_e^{mod}\right\}. \tag{3}$$

III. Problem Formulation for the Optimal Battery Cell/Module Reconfiguration

To shorten the BCE time of a given system, significant research efforts have been directed to improve the circuit designs, connection topologies, and control strategies of battery charge equalizers. However, the influence of battery cell/module configuration on battery charge balance or equalization has not been well investigated so far. Indeed, for a module-based BCE system, the BCE time may vary dramatically if we change the configuration of the battery cells/modules. Motivated by this, in this section we first review the circuit designs for battery reconfiguration, and then formulate the optimization problems to minimize the BCE time of module-based BCE systems under two reconfiguration levels of battery cells/modules.

A. Circuit Designs for Reconfigurable Battery Systems

In multi-cell reconfigurable battery systems, battery cells can be connected in different topologies to meet various requirements of charging/discharging current/voltage/power/capacity. To do so, several circuit designs for battery system reconfiguration have been proposed and patented [27]–[30]. For instance, in the reconfigurable battery systems designed in [27]–[29], a selectable number of battery modules/cells could be connected either in series or parallel by switch operations to meet different load or charger requirements. For large-scale battery systems, a dynamic reconfiguration framework was presented in [30]. In principle, to reconfigure a battery system, one can either relocate the battery cells or change their connection wiring. While it may not be feasible to frequently relocate battery cells, the connection topology could be flexibly adjusted through rewiring or switching circuit designs. In some typical reconfigurable battery designs, six controllable switches are attached to each battery cell to facilitate the series, parallel, or mixed connections of all battery cells [12], [13]. As a result, dynamic operation of individual battery cells becomes possible, which leads to higher efficiency and improved reliability. The cost of switching circuit designs mainly depends on the number of switches applied. To further reduce the cost, two-switch [14] and single-switch [31] designs have also been developed. While the number of switches per cell is reduced for lower cost and system complexity, the level of system reconfigurability is compromised. Next, we will first analyze different levels of reconfigurability of the module-based BCE system, and then introduce how to formulate the problems for optimal battery cell/module configuration and discuss its complexity.

B. Levels of Reconfigurability

In a module-based BCE system, both cell reconfiguration and module reconfiguration may be achievable through different circuit designs. Here, we consider the following three types of battery reconfigurations:

- *Module reconfiguration:* The connecting sequence of all battery modules can be changed.
- *Intra-module cell reconfiguration:* The connecting sequence of all cells in a single module can be changed. However, a cell is not allowed to be relocated from its original module to other modules.
- *Inter-module cell reconfiguration:* A cell can be reconfigured to any module, but the total number of modules and the total number of cells per module do not change.

Clearly, while the intra-module cell reconfiguration only involves battery cells within one module, the inter-module cell reconfiguration is implemented among all battery cells and thus it requires more connection flexibility. Because of permutation effects, it also leads to orders of magnitude greater number of possible configurations, which severely adds complexity to the optimization of the battery cell/module configuration for fast charge equalization.

In the following, we consider two general levels of reconfigurability in the module-based BCE system:

- *Bounded Reconfiguration (BR):* Module reconfiguration and intra-module cell reconfiguration are allowed, but inter-module cell reconfiguration is forbidden;

- *Complete Reconfiguration (CR):* Module reconfiguration, intra-module cell reconfiguration, and inter-module cell reconfiguration are all allowed.

C. Minimizing the BCE Time by BR

As discussed in Section II-A, the module-based BCE system consisting of M modules can be viewed as $M+1$ independently operating series-based BCE subsystems. Denote the configuration of the m-th subsystem by a vector $\mathbf{C}_\mathbf{B}^m$, $m \in \{1, \ldots, M+1\}$. In the cell configuration, each cell is represented by its initial SOC such that, for instance, a cell configuration $\mathbf{C}_\mathbf{B}^2 = [0.60, 0.57, 0.62]$ indicates that in the second subsystem three cells with initial SOCs 0.60, 0.57, and 0.62 are connected in series in the corresponding order. Particularly, the module configuration, i.e., $\mathbf{C}_\mathbf{B}^{M+1}$, is defined by a vector composed of all cell configurations. For example, a module-based BCE system with $M = 3$ modules has several possible module configurations, such as $\mathbf{C}_\mathbf{B}^4 = [\mathbf{C}_\mathbf{B}^2, \mathbf{C}_\mathbf{B}^3, \mathbf{C}_\mathbf{B}^1]$ or $\mathbf{C}_\mathbf{B}^4 = [\mathbf{C}_\mathbf{B}^3, \mathbf{C}_\mathbf{B}^1, \mathbf{C}_\mathbf{B}^2]$. Note that, $\mathbf{C}_\mathbf{B}^m$ is a variable and $\mathbf{C}_\mathbf{B}^m \in \mathbf{S}_\mathbf{B}^m$, where $\mathbf{S}_\mathbf{B}^m$ is the set of all possible configurations of the m-th subsystem to be considered.

Then, the BCE time corresponding to the subsystem configuration $\mathbf{C}_\mathbf{B}^m$ is denoted by $T_e(\mathbf{C}_\mathbf{B}^m)$, $m \in \{1, \ldots, M+1\}$, which can be calculated using (1) or (2), i.e., the BCE time calculation formula for the series-based BCE system. Besides, the entire system's BCE time corresponding to all these subsystem configurations is denoted by $T_e^{sys}(\mathbf{C}_\mathbf{B}^1, \ldots, \mathbf{C}_\mathbf{B}^{M+1})$, which can be calculated using (3). Clearly, the BCE time depends on the system configuration. In order to evaluate the minimum BCE time of a module-based BCE system including M modules, based on (3), the following optimization problem is formulated:

$$\min_{\substack{\mathbf{C}_\mathbf{B}^m \in \mathbf{S}_\mathbf{B}^m \\ m=1,\ldots,M+1}} T_e^{sys}\left(\mathbf{C}_\mathbf{B}^1, \ldots, \mathbf{C}_\mathbf{B}^{M+1}\right) = \min_{\substack{\mathbf{C}_\mathbf{B}^m \in \mathbf{S}_\mathbf{B}^m \\ m=1,\ldots,M+1}} \left\{ \max_{i \in \{1,\ldots,M+1\}} T_e^{sub}\left(\mathbf{C}_\mathbf{B}^i\right) \right\}. \quad (4)$$

In the above problem (4), the subsystem configurations $\mathbf{C}_\mathbf{B}^i$, $i \in \{1, \ldots, M+1\}$, are optimization variables subject to constraints $\mathbf{C}_\mathbf{B}^i \in \mathbf{S}_\mathbf{B}^i$, and $T_e^{sub}(\mathbf{C}_\mathbf{B}^i)$ relates these optimization variables to the objective function based on (1) and (2), i.e.,

$$T_e^{sub}\left(\mathbf{C}_\mathbf{B}^i\right) = \begin{cases} T_e^{cel}(i), & \text{if } 1 \le i \le M, \\ T_e^{mod}, & \text{if } i = M+1. \end{cases}$$

When performing the BR, each battery cell or module is bounded within its original subsystem, i.e., the component cells/modules of each subsystem remain unchanged while their connection sequence is reconfigured. Thus, the reconfiguration of each subsystem can be carried out independently. As a result, under the BR, the objective function in the optimization problem (4) can be simplified to:

$$\min_{\substack{\mathbf{C}_\mathbf{B}^m \in \mathbf{S}_\mathbf{B}^m \\ m=1,\ldots,M+1}} T_e^{sys}\left(\mathbf{C}_\mathbf{B}^1, \ldots, \mathbf{C}_\mathbf{B}^{M+1}\right) = \min_{\substack{\mathbf{C}_\mathbf{B}^m \in \mathbf{S}_\mathbf{B}^m \\ m=1,\ldots,M+1}} \left\{ \max_{i \in \{1,\ldots,M+1\}} T_e^{sub}\left(\mathbf{C}_\mathbf{B}^i\right) \right\}$$

$$= \max_{i \in \{1,\ldots,M+1\}} \left\{ \min_{\mathbf{C}_\mathbf{B}^i \in \mathbf{S}_\mathbf{B}^i} T_e^{sub}\left(\mathbf{C}_\mathbf{B}^i\right) \right\}. \quad (5)$$

Then, in order to find the shortest BCE time of the entire system under the BR, we only need to search for the shortest BCE time of each subsystem. Thus, according to (5), to find the shortest BCE time of a module-based BCE system including M modules and B cells per module, the total number of different subsystem configurations to be tested under the BR is

$$N_{BR} = \frac{B!}{2} \times M + \frac{M!}{2}. \quad (6)$$

Note that, since a cell/module configuration and its reverse have the same BCE time, we do not test the reversed ones.

D. Minimizing the BCE Time by CR

When the CR is carried out, battery cells could be relocated to any place in the battery series while the total number of modules in the system, i.e., M, and the total number of cells per module, i.e., B, do not change. This is more complicated than the BR since the reconfiguration in one subsystem may affect those in other subsystems. The CR can be implemented in two steps: first dividing the set consisting of all $M \times B$ battery cells evenly into M modules (subsets) with B cells per module to form an *equal-size cell partition*, denoted by P_{ar}, and then performing the BR with all battery cells bounded within their own modules (subsets) according to the generated P_{ar}. Note that, the equal-size cell partition $P_{ar} \in S_P$ is a variable, where S_P is the full set of all equal-size cell partitions. Then, the total number of possible equal-size cell partition $P_{ar} \in S_P$ is

$$N_{P_{ar}} = \binom{MB}{B} \times \binom{MB-B}{B} \times \cdots \times \binom{B}{B} \times \frac{1}{M!} = \frac{(MB)!}{M!(B!)^M}. \quad (7)$$

According to (6) and (7), in order to search for the shortest system BCE time, the total number of different configurations to be tested under the CR is

$$N_{CR} = N_{P_{ar}} \times N_{BR} = \frac{(MB)!}{M!(B!)^M} \times \left(\frac{B!}{2} \times M + \frac{M!}{2} \right). \quad (8)$$

Given any equal-size cell partition $P_{ar} \in S_P$ generated at the first step, the m-th subsystem configuration constructed based on the subsets of P_{ar} is denoted by $\mathbf{C}_\mathbf{B}^m(P_{ar}) \in \mathbf{S}_\mathbf{B}^m(P_{ar})$, $m \in \{1, \ldots, M+1\}$, where $\mathbf{S}_\mathbf{B}^m(P_{ar})$ is the full set of all possible configurations of $\mathbf{C}_\mathbf{B}^m(P_{ar})$. Thus, under the CR, by extending (5), we need to solve the following problem for the minimum system BCE time:

$$\min_{P_{ar} \in S_P} \min_{\substack{\mathbf{C}_\mathbf{B}^m(P_{ar}) \in \mathbf{S}_\mathbf{B}^m(P_{ar}) \\ m=1,\ldots,M+1}} T_e^{sys}\left(\mathbf{C}_\mathbf{B}^1(P_{ar}), \ldots, \mathbf{C}_\mathbf{B}^{M+1}(P_{ar})\right) = \min_{P_{ar} \in S_P} \max_{i \in \{1,\ldots,M+1\}} \min_{\mathbf{C}_\mathbf{B}^i(P_{ar}) \in \mathbf{S}_\mathbf{B}^i(P_{ar})} T_e^{sub}\left(\mathbf{C}_\mathbf{B}^i(P_{ar})\right). \quad (9)$$

In the above problem (9), both the equal-size cell partition P_{ar} and the generated subsystem configuration $\mathbf{C}_\mathbf{B}^i(P_{ar})$, $i \in \{1, \ldots, M+1\}$, are optimization variables, and they are subject to constraints $P_{ar} \in S_P$ and $\mathbf{C}_\mathbf{B}^i(P_{ar}) \in \mathbf{S}_\mathbf{B}^i(P_{ar})$.

In order to solve the optimization problems (5) and (9) for the minimum BCE time of a module-based BCE system, a straightforward way is exhaustive search, i.e., try all possible cell/module configurations and identify the one yielding the shortest BCE time. However, as one can easily see from (6) and (8), as the system size increases, i.e., B and/or M increase, the total number of subsystem configurations to be tested grows very fast since they are functions of factorials. For example, for a system with $M = 6$ and $B = 8$, if the CR is performed, the total number of configurations can reach about 4.868×10^{35} according to (8). Even for the BR, the total number of configurations still goes to 121,320 according to (6). Thus, for large-scale systems, it becomes infeasible to use the exhaustive search for identifying the cell/module configuration with the shortest BCE time. Therefore, computationally efficient battery reconfiguration algorithms are needed to achieve the minimum or near-minimum BCE time under different levels of reconfigurability. This will be studied in Sections IV and V for module-based BCE systems under the Bounded and Complete Reconfigurations, respectively.

IV. Optimal Cell/Module Configuration Under the Bounded Reconfiguration

A. Module-Based Bounded Reconfiguration Algorithm

Consider a module-based BCE system under the BR. Again, such a system can be viewed as $M + 1$ reconfigurable series-based BCE subsystems. According to the BCE time calculation formula (3), we can calculate the BCE time of each subsystem, and then select the longest one as the entire system's BCE time T_e^{sys}. Thus, to achieve a shorter T_e^{sys}, we need to focus on the subsystem resulting in the longest BCE time. For such a reconfigurable series-based BCE subsystem, an algorithm was developed in our prior work [25] to identify the battery cell configuration leading to the near-shortest BCE time, and it is referred to as the *series-based reconfiguration algorithm* in this paper. Based on this algorithm, we propose the *module-based BR algorithm* to minimize the BCE time of module-based BCE systems as follows.

Module-based BR algorithm:

Step 1: Calculate the BCE time of each series-based BCE subsystem in the module-based BCE system using (1) or (2), and select the subsystem leading to the longest BCE time as the *critical subsystem*.

Step 2: If any subsystem is selected as the critical subsystem for the second time, output the final cell/module configuration and terminate the algorithm. Otherwise, go to Step 3.

Step 3: Apply the series-based reconfiguration algorithm to the critical subsystem to minimize its BCE time. Then return to Step 1.

B. Illustration of the Calculation Accuracy of the BCE Time

As we can see, the above module-based BR algorithm is derived and carried out based on the BCE time calculation formulas (1)-(3). To illustrate the calculation accuracy of the BCE time using (1)-(3), we collect experimental data for the module-based BCE system from the same testbed used in [32] as shown in Fig. 3. Specifically, the battery charge equalization is tested in a down-scaled system for illustration, i.e., a module-based BCE system composed of $M = 3$ modules and $B = 2$ cells per module. In this system, Sony VTC4 18650 Lithium battery cells with a rated charge capacity of 2100 mAh are installed. Besides, as the key component performing charge equalization, the battery charge equalizer is designed based on a modified buck-boost converter composed of a 3.46 μH WE-FB Flyback transformer, two NTD6416AN-1G MOSFETs, and two 0.1 Ω current sense resistors. Such charge equalizers are applied to both the cell-level and module-level charge transfers in the module-based BCE system, as shown in Fig. 2. Using this testbed, given the initial cell SOCs and parameter values, we can obtain the experimental data of the cell SOC evolution throughout the charge equalization process.

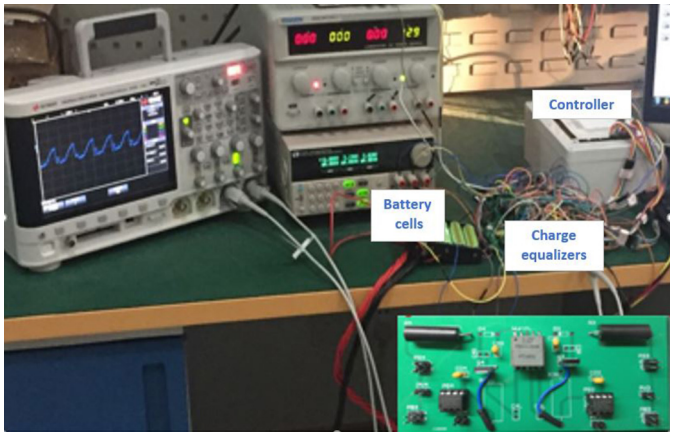

Fig. 3. The testbed for circuit experiments.

The original cell configuration is [(0.78,0.80), (0.72,0.76), (0.73,0.74)]. After applying the proposed module-based BR algorithm, the obtained configuration is [(0.72,0.76), (0.78,0.80), (0.73,0.74)]. Then, the original and proposed configurations are tested by circuit experiments and their cell SOC evolutions and BCE times are compared in Fig. 4. During the charge equalization process, the average equalization current between battery cells is about 0.261 A. When higher equalization current is applied, the charge transfer rates are increased and the resultant BCE time is expected to be shortened according to the BCE time calculation formulas (1)-(3).

As shown in Fig. 4, the original configuration and that generated by the proposed module-based BR algorithm yield BCE times of 1,090 s and 605 s, respectively. When using formulas (1)-(3) based on the average charge transfer rates and loss rates from circuit experiments, the calculated BCE times are 1,103 s for the original configuration and 611 s for the generated configuration. Then the corresponding absolute percentage errors are 1.19% and 0.99%. Thus, the calculation formulas (1)-(3) can provide an accurate estimation of the BCE time of the module-based BCE system. Such high calculation accuracy also indicates that it is appropriate to represent the charge transfer rates and loss rates by their average rates since they both vary within narrow ranges.

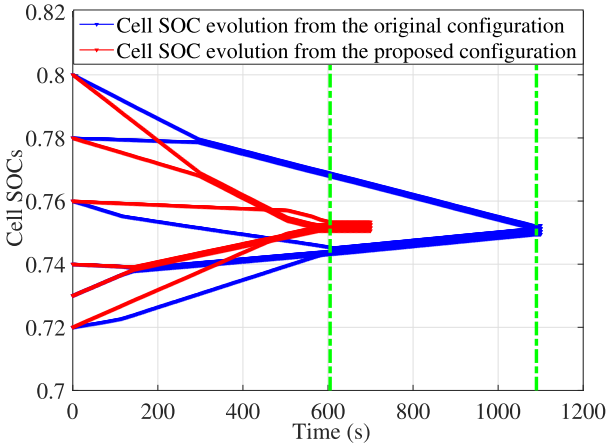

Fig. 4. The cell SOC evolution and BCE time of the original configuration and the configuration obtained from the module-based BR algorithm based on circuit experiment data.

Fig. 4 also illustrates that the BCE time can vary dramatically between different system configurations. Then, we are motivated to develop the reconfiguration algorithm generating a system configuration with the shortest BCE time, i.e., the fastest charge equalization. To evaluate its optimality, we need to compare the BCE time of the generated configuration with the shortest one. To identify the shortest BCE time, typically all possible configurations need to be tested. To do so, while circuit experiments become too time- and energy-consuming, the formulas (1)-(3) demonstrating sufficient accuracy are much more efficient [22]. Thus, in the subsequent study requiring a large number of tests, the calculation formulas (1)-(3) will be used to evaluate the BCE times of various battery cell/module configurations.

C. Optimality and Computational Efficiency

To evaluate the optimality of the proposed module-based BR algorithm on larger systems under various cell/module configurations, we compare the BCE times obtained from the proposed algorithm and the exhaustive search by numerical experiments. Specifically, for a module-based BCE system with $M = 6$ modules and $B = 8$ cells per module, a total of S =10,000 initial cell SOC test cases are generated following the uniform distribution $U(0, 1)$.

According to (6), for the s-th test case generated, a total of 121,320 possible configurations need to be tested in the exhaustive search. Of all BCE times of these configurations, the minimum is denoted by $T_e^{exh}(s)$. Let the corresponding BCE time obtained by the proposed module-based BR algorithm be denoted by $T_e^{BR}(s)$. To evaluate the optimality of the proposed algorithm, we define the percentage difference in BCE time, as well as its mean and maximum, as follows.

$$\epsilon_d(s) = \frac{T_e^{BR}(s) - T_e^{exh}(s)}{T_e^{exh}(s)} \times 100\%, \quad s = 1, 2, \ldots, S,$$

$$\bar{\epsilon}_d = \frac{1}{S}\sum_{s=1}^{S} \epsilon_d(s), \ \epsilon_d^{max} = \max_{s\in\{1,2,\ldots,S\}} \epsilon_d(s).$$

TABLE I
COMPARISON OF BCE TIMES AND COMPUTATION TIMES OF THE PROPOSED MODULE-BASED BR ALGORITHM AND EXHAUSTIVE SEARCH FOR 10,000 TEST CASES OF A 48-CELL MODULE-BASED BCE SYSTEM

$\bar{\epsilon}_d$	ϵ_d^{max}	r_{suc}	$\overline{T}_{com}^{exh}$	$\overline{T}_{com}^{BR}$	$\overline{T}_{com}^{BR}/\overline{T}_{com}^{exh} \times 100\%$
0.025%	9.298%	98.800%	8.165 s	2.605 s	31.904%

To quantify the success rate at which the proposed algorithm also leads to the minimum BCE time, we define

$$r_{suc} = \frac{\text{Total number of test cases with } T_e^{BR}(s) = T_e^{exh}(s)}{S}.$$

In addition to the optimality of the proposed algorithm, we also evaluate its computational efficiency by comparing the computation times of the exhaustive search and the proposed algorithm, which are denoted as $T_{com}^{exh}(s)$ and $T_{com}^{BR}(s)$, respectively. Their means are

$$\overline{T}_{com}^{exh} = \frac{1}{S}\sum_{s=1}^{S} T_{com}^{exh}(s), \ \overline{T}_{com}^{BR} = \frac{1}{S}\sum_{s=1}^{S} T_{com}^{BR}(s).$$

Then, these performance measures are summarized and compared in Table I. As we can see, for such a module-based BCE system, the proposed algorithm can result in the minimum BCE time in 98.8% test cases, while its average computation time is only 31.904% of that of the exhaustive search. In addition, while the proposed algorithm fails to identify the configuration with the minimum BCE time in 1.2% of the test cases, the resulting BCE time is only 0.025% longer than the minimum on average. Therefore, the proposed module-based BR algorithm can lead to a near-minimum BCE time, but requires much less computational efforts than the exhaustive search.

V. Optimal Cell/Module Reconfiguration Under the Complete Reconfiguration

In the CR of a module-based BCE system, battery cells can be reconfigured to any position of the battery string. As a result, the number of possible configurations is orders of magnitude larger than that under the BR. Thus, the BCE time should have the potential to be further improved. Motivated by this, we extend our investigation to systems under the CR.

As discussed in Section III, to perform the CR, we can take two steps. At the first step, the set composed of all $M \times B$ battery cells is divided into M modules (subsets) with each module having B cells (elements). Thus, the resultant system from this step is an equal-size cell partition, i.e., each module of the cell partition contains the same number of cells. Note that, at this step, neither the cell connection sequence in each module nor the module sequence in the module-based system (equal-size cell partition) matters. Then, at the second step, for each equal-size cell partition, all cells are bounded within their original modules assigned in the first step, and thus the module-based BR algorithm proposed in Section IV can be used to determine the cell order within each module as well as the module order. Therefore, in this section, we will focus

on the first step and discuss approaches to generate equal-size cell partitions.

A. Equal-Size Cell Partition

Clearly, finding an equal-size cell partition of good quality is critical under the CR. However, this is challenging since, according to (8), the total number of equal-size cell partitions is $\frac{(MB)!}{M!(B!)^M}$ for a system with M modules and B cells in each module. As the system size increases, the total number of equal-size cell partitions grows very fast. For instance, given $M = 6$ and $B = 8$, the total number of equal-size cell partitions is 4.0129×10^{30}. Therefore, a computationally efficient method is necessary to help us quickly identify a high-quality equal-size cell partition.

According to (3), the BCE time of a module-based BCE system is the longest one of all its subsystems' BCE times. Intuitively, if all cell SOCs in the m-th module are close to each other, we can get a small $T_e^{cel}(m)$. On the other hand, if the total cell SOCs of each module get closer to each other, T_e^{mod} will become smaller. Following this idea, we propose three approaches to construct the equal-size cell partition aiming at short $T_e^{cel}(m)$ and/or T_e^{mod} as follows.

Approach 1 to reduce all cell-level BCE times $T_e^{cel}(m)$: Sort all cells in descending SOC order and then assign the cell series consisting of the $((m-1)B+1)$-th cell to the mB-th cell into the m-th module, $m \in \{1, 2, \ldots, M\}$.

Approach 2 to reduce the module-level BCE time T_e^{mod}:

Step 1: Sort all cells in descending SOC order and assign the m-th cell into the m-th module, $m \in \{1, 2, \ldots, M\}$.

Step 2: Calculate each module's total cell SOC by summing up the SOCs of all cells already assigned to the module, and sort all modules by their total cell SOCs.

Step 3: Pick up the first M cells from the remaining unassigned cells and assign the cell with the m-th largest SOC into the module with the m-th smallest total cell SOC, $m \in \{1, 2, \ldots, M\}$.

Step 4: If all cells have been assigned into battery modules, terminate the algorithm. Otherwise, return to Step 2.

Approach 3 to balance $T_e^{cel}(m)$ and T_e^{mod}: Step 1, 2, and 4 are same to those in Approach 2. Only replace Step 3 in Approach 2 by:

Step 3′: Pick up the first M cells from the remaining unassigned cells and assign the cell with the m-th largest SOC into the module with the m-th **largest** total cell SOC, $m \in \{1, 2, \ldots, M\}$.

To compare the performance of these three approaches, we test each approach using the same $S = 10{,}000$ initial cell SOC test cases randomly generated in Section IV-C. For the s-th case, $s \in \{1, 2, \ldots, S\}$, the BCE times of the cell/module configurations with equal-size partition generated based on Approaches 1, 2, and 3 are denoted by $T_e^{app1}(s)$, $T_e^{app2}(s)$, and $T_e^{app3}(s)$, respectively. In addition, for the s-th case, the BCE time $T_e^{exh}(s)$ obtained from the exhaustive search under the BR in Section IV-C is used here for reference. Then for the $S = 10{,}000$ test cases, $T_e^{app1}(s)$, $T_e^{app2}(s)$, and $T_e^{app3}(s)$, are compared with $T_e^{exh}(s)$ in Figure 5.

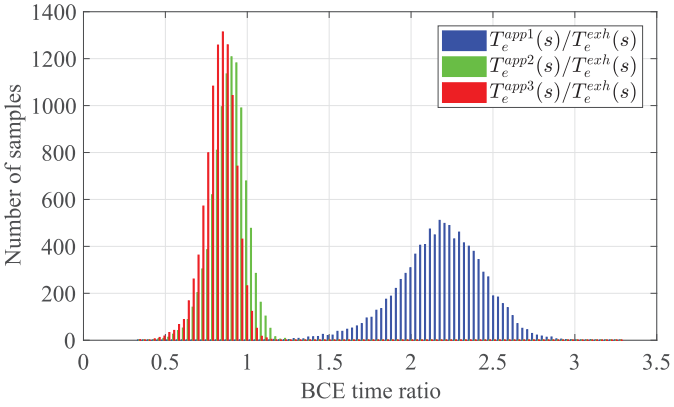

Fig. 5. Comparison of the ratios of the BCE times achieved by three approaches of generating equal-size cell partitions and the BCE time obtained from the exhaustive search under the BR.

Based on Figure 5 and the numerical simulation results, $\frac{T_e^{app1}(s)}{T_e^{exh}(s)} > 1$ in 99.97% of all test cases, i.e., Approach 1 almost always fails to beat the optimal configuration under the BR. On the other hand, $\frac{T_e^{app2}(s)}{T_e^{exh}(s)} < 1$ in 87.20% of all cases and $\frac{T_e^{app3}(s)}{T_e^{exh}(s)} < 1$ in 97.59% of all cases. In other words, it is highly possible that the BCE time can be improved if Approach 2 or Approach 3 is applied. In addition, since the BCE times obtained from Approach 3 are shorter than those from Approach 2 in 92.19% of all cases, we will apply Approach 3 to generate the equal-size cell partition in the subsequent analysis. Then, the entire module-based CR algorithm is described by a flowchart as shown in Fig. 6.

B. Optimality and Computational Efficiency

Based on the above analysis, for module-based BCE systems under the CR, we develop the *module-based CR algorithm* consisting of Approach 3 for generating equal-size cell partitions as the first step and the module-based BR algorithm proposed in Section IV as the second step. To test its optimality, we need to compare the BCE time obtained from the proposed algorithm with the minimum BCE time. However, to solve the optimization problem (9) for the minimum BCE time under the CR, exhaustive search becomes impractical when $M > 4$ and $B > 4$. Thus, we have to use other optimization tools, such as the genetic algorithm (GA), to evaluate the minimum BCE time. Although GA cannot guarantee a global minimum, it is commonly used to get high-quality solutions to optimization problems [33].

When using GA to estimate the minimum BCE time, the initial population is generated randomly and a total of 60 individuals are generated for every generation. In addition, the GA is terminated if the resulting BCE time stays unimproved for 10^6 generations, or it reaches the computation time upper limit, i.e., 2 hours, or the total number of generations exceeds 5×10^8. For the module-based system with $M = 6$ modules and $B = 8$ cells in each module, we generate $S = 1000$ initial 48-cell SOC test cases following the uniform distribution

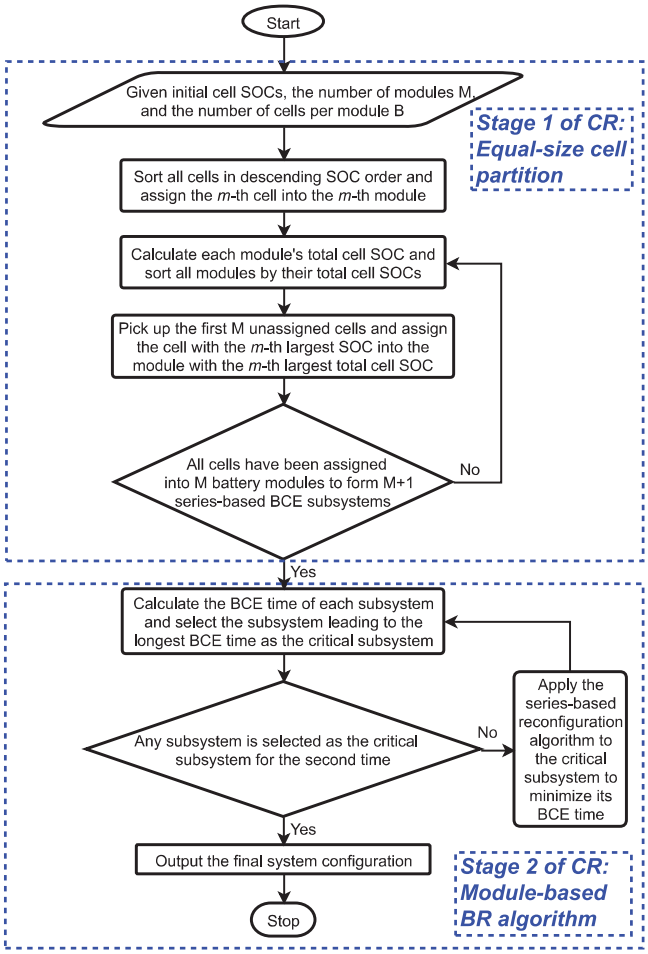

Fig. 6. A flowchart of the module-based CR algorithm.

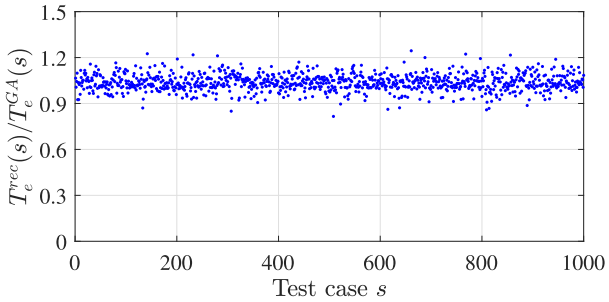

Fig. 7. BCE time ratios of the proposed module-based CR algorithm and GA for 1000 randomly generated initial cell SOC test cases of a module-based BCE system with 6 modules and 8 cells per module.

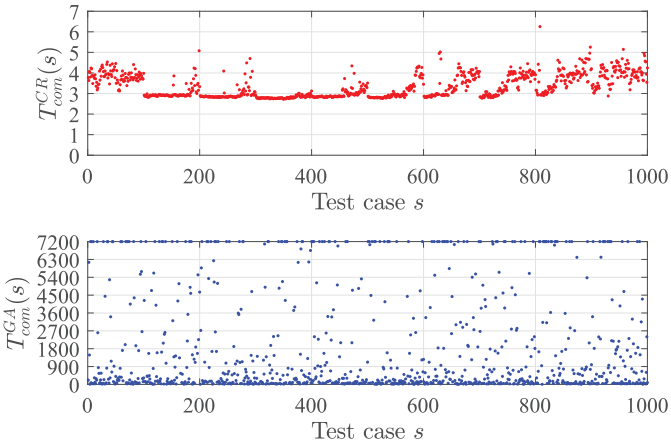

Fig. 8. Comparison of the computation times of the proposed module-based CR algorithm and GA when they reach the same BCE times for 1000 randomly generated initial cell SOC test cases of a module-based BCE system with 6 modules and 8 cells per module.

$U(0, 1)$. For any configuration of each test case, the BCE time is calculated based on (1)-(3).

First, we investigate the optimality of the proposed module-based CR algorithm by comparing its BCE time with that obtained by the GA. For the s-th test case, $s = 1, 2, \ldots, S$, the BCE times obtained from the module-based CR algorithm and GA are denoted by $T_e^{CR}(s)$ and $T_e^{GA}(s)$, respectively. For all $S = 1000$ test cases, as shown in Fig. 7, the BCE time ratios $T_e^{CR}(s)/T_e^{GA}(s)$ ranges from 0.816 to 1.244 with a mean of 1.038. Thus, for these 1000 randomly generated test cases, the BCE times obtained from the proposed algorithm are similar to the minimum BCE times obtained by the GA.

Since the proposed algorithm and the GA perform similarly in terms of BCE times, it becomes most important how their computational requirements differ. Therefore, we also compare the computation times of the proposed module-based CR algorithm and the GA when they both reach the same BCE time level. For the s-th test cases studied, the computation time of the proposed CR algorithm and that of the GA are denoted by $T_{com}^{CR}(s)$ and $T_{com}^{GA}(s)$, respectively, and they are compared in Fig. 8. Note that, the GA is terminated once it achieves the same BCE time level of the proposed CR algorithm or its computation time reaches 2 hours. According to the simulation results, the GA succeeds in achieving the same BCE time of the proposed reconfiguration in 81.2% of all cases. However, the average computation time of the proposed module-based CR algorithm is 3.33 s while that of GA is about 2,147.83 s. Thus, to reach the same BCE time level, the proposed module-based CR algorithm is far more computationally efficient than the GA.

Therefore, as compared to GA, the proposed module-based CR algorithm can provide an optimal or near-optimal BCE time with much less computation time.

C. Comparison With Industrial Solutions

In order to demonstrate the efficacy of the proposed algorithms, we also compare the resultant BCE times with those obtained from some industrial solutions. In industrial practice, some simple reconfiguration methods are applied based on certain heuristics. For instance, it is quite common to perform charge balance by directly connecting a charge equalizer to the two cells/modules with largest deviations above and below the average cell SOC, which is referred to as the *largest deviation-based reconfiguration* (*LDR*). This can be carried out step by step until all battery cells are involved, as illustrated in Fig. 9 for a small 6-cell system with the initial cell SOCs given in Fig. 4.

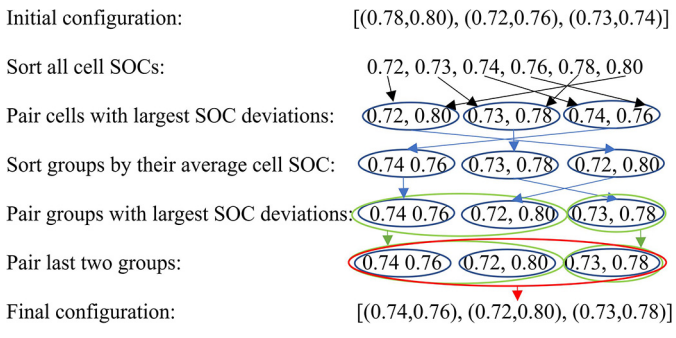

Fig. 9. Illustration of the reconfiguration based on the largest SOC deviation.

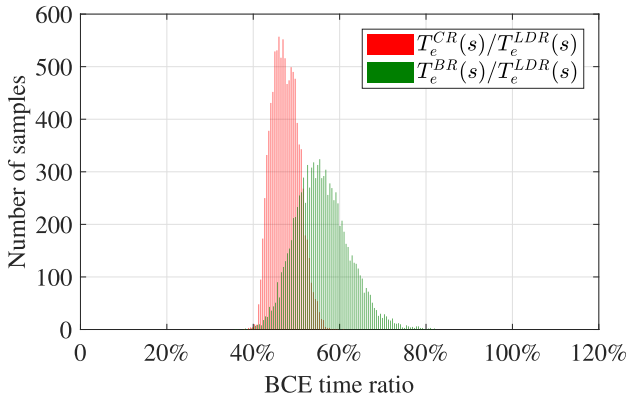

Fig. 10. Ratios of BCE times resulting from the module-based CR, BR algorithms and the LDR.

Then, we compare the ratios of BCE times resulting from the proposed module-based CR, BR algorithms and the industrial solution LDR in Fig. 10 using the S=10,000 initial cell SOC test cases randomly generated in Section IV-C for the 48-cell module-based BCE system. Clearly, for each test case s, $s = 1, 2, \ldots, S$, the BCE times obtained from the proposed module-based CR and BR algorithms, i.e., $T_e^{CR}(s)$ and $T_e^{BR}(s)$, respectively, are always shorter than that resulting from the LDR, i.e., $T_e^{LDR}(s)$. Specifically, for these test cases, the average ratios $\overline{T_e^{CR}(s)/T_e^{LDR}(s)} = 47.498\%$ and $\overline{T_e^{BR}(s)/T_e^{LDR}(s)} = 55.882\%$. Thus, as compared to the industrial solution of LDR, the proposed algorithms can help dramatically expedite the BCE process.

VI. Conclusion and Future Work

In this work, we explore the influence of battery cell/module configuration on the speed of battery charge equalization in module-based BCE systems. For different levels of reconfigurability, the module-based BR and CR algorithms are proposed. As compared to the exhaustive search and/or genetic algorithm, the proposed algorithms are capable of identifying the configuration leading to the minimum or near-minimum BCE times with much shorter computation time.

In addition to the optimal BCE time studied in this paper, other important performance measures, e.g., energy efficiency and system reliability, will be investigated in our future work. Besides, in this paper, the optimal cell/module configuration is determined and set up before the battery charge is balanced. We will extend our study to dynamic and adaptive cell/module reconfiguration during the charge balance process for further improved system performance. Moreover, a more practical circuit testbed will be designed to facilitate the validation of the proposed algorithms.

While this paper is focused on BCE systems based on cell-to-cell charge equalization, other BCE structures based on cell-to-pack or pack-to-cell battery equalizers, can be similarly investigated in the future by adaptively applying the analysis procedure and relevant results obtained in this paper.

References

[1] M. Anderman. (2014). *Tesla Motors: Battery Technology, Analysis of the Gigafactory, and the Automakers Perspectives*. [Online]. Available: http://www.advancedautobat.com/industry-reports/2014-Tesla-report/Extract-from-the-Tesla-battery-report.pdf

[2] *Global Energy Storage Database*. Accessed: May 1, 2018. [Online]. Available: https://www.energystorageexchange.org/projects

[3] G. Wang, J. Pou, and V. G. Agelidis, "Reconfigurable battery energy storage system for utility-scale applications," in *Proc. IEEE Annu. Conf. Ind. Electron. Soc.*, Nov. 2015, pp. 86–91.

[4] W. F. Bentley, "Cell balancing considerations for lithium-ion battery systems," in *Proc. 12th Annu. Battery Conf. Appl. Adv.*, Jan. 1997, pp. 223–226.

[5] J. Kim, J. Shin, C. Chun, and B. H. Cho, "Stable configuration of a Li-Ion series battery pack based on a screening process for improved voltage/SOC balancing," *IEEE Trans. Power Electron.*, vol. 27, no. 1, pp. 411–424, Jan. 2012.

[6] S. Wen, "Cell balancing buys extra run time and battery life," *Anal. Appl. J.*, vol. 1, pp. 14–18, 2009.

[7] Y. Barsukov, *Battery Cell Balancing: What to Balance and How*, Portable Power Design Seminar, Texas Instrum., Dallas, TX, USA, 2006.

[8] J. Gallardo-Lozano, E. Romero-Cadaval, M. I. Milanes-Montero, and M. A. Guerrero-Martinez, "Battery equalization active methods," *J. Power Sources*, vol. 246, pp. 934–949, Jan. 2014.

[9] K. Zhi-Guo, Z. Chun-Bo, L. Ren-Gui, and C. Shu-Kang, "Comparison and evaluation of charge equalization technique for series connected batteries," in *Proc. IEEE Power Electron. Specialists Conf.*, Jun. 2006, pp. 1–6.

[10] S. Ci, N. Lin, and D. Wu, "Reconfigurable battery techniques and systems: A survey," *IEEE Access*, vol. 4, pp. 1175–1189, 2016.

[11] L. He *et al.*, "Exploring adaptive reconfiguration to optimize energy efficiency in large-scale battery systems," in *Proc. IEEE 34th Real Time Syst. Symp.*, Dec. 2013, pp. 118–127.

[12] S. Ci, J. Zhang, H. Sharif, and M. Alahmad, "A novel design of adaptive reconfigurable multicell battery for power-aware embedded networked sensing systems," in *Proc. IEEE Glob. Telecommun. Conf.*, Nov. 2007, pp. 1043–1047.

[13] H. Kim and K. G. Shin, "On dynamic reconfiguration of a large-scale battery system," in *Proc. 15th IEEE Real Time Embedded Technol. Appl. Symp.*, Apr. 2009, pp. 87–96.

[14] T. Kim, W. Qiao, and L. Qu, "Series-connected self-reconfigurable multicell battery," in *Proc. 26th Annu. IEEE Appl. Power Electron. Conf. Exposit.*, Mar. 2011, pp. 1382–1387.

[15] H. Kim and K. G. Shin, "Scheduling of battery charge, discharge, and rest," in *Proc. 30th IEEE Real Time Syst. Symp.*, Dec. 2009, pp. 13–22.

[16] L. He *et al.*, "RAC: Reconfiguration-assisted charging in large-scale lithium-ion battery systems," *IEEE Trans. Smart Grid*, vol. 7, no. 3, pp. 1420–1429, May 2016.

[17] L. He *et al.*, "SoH-aware reconfiguration in battery packs," *IEEE Trans. Smart Grid*, vol. 9, no. 4, pp. 3727–3735, Jul. 2018.

[18] J. Cabrera, A. Vega, F. Tobajas, V. Déniz, and H. A. Fabelo, "Design of a reconfigurable li-ion battery management system (BMS)," in *Proc. Technol. Appl. Electron. Teach.*, Jun. 2014, pp. 1–6.

[19] J. Cao, N. Schofield, and A. Emadi, "Battery balancing methods: A comprehensive review," in *Proc. IEEE Veh. Power Propulsion Conf.*, Sep. 2008, pp. 1–6.

[20] M. Daowd, N. Omar, P. Van den Bossche, and J. Van Mierlo, "Passive and active battery balancing comparison based on MATLAB simulation," in *Proc. IEEE Veh. Power Propulsion Conf.*, Sep. 2011, pp. 1–7.

[21] W. Han and L. Zhang, "Charge transfer and energy transfer analysis of battery charge equalization," in *Proc. IEEE Int. Conf. Autom. Sci. Eng.*, Aug. 2015, pp. 1137–1138.
[22] W. Han, C. Zou, C. Zhou, and L. Zhang, "Estimation of cell SOC evolution and system performance in module-based battery charge equalization systems," *IEEE Trans. Smart Grid*, to be published.
[23] (2017). *SDG&E Unveils World's Largest Lithium Ion Battery Storage Facility*. [Online]. Available: http://sdgenews.com/battery-storage/sdge-unveils-world's-largest-lithium-ion-battery-storage-facility
[24] W. Han, L. Zhang, and Y. Han, "Mathematical modeling, performance analysis and control of battery equalization systems: Review and recent developments," in *Advances in Battery Manufacturing, Services, and Management Systems*, J. Li, S. Zhou, and Y. Han, Eds. New York, NY, USA: Wiley, 2016, ch. 12, pp. 281–301.
[25] W. Han and L. Zhang, "Battery cell reconfiguration to expedite charge equalization in series-connected battery systems," *IEEE Robot. Autom. Lett.*, vol. 3, no. 1, pp. 22–28, Jan. 2018.
[26] W. Han, L. Zhang, and Y. Han, "Computationally efficient methods for state of charge approximation and performance measure calculation in series-connected battery equalization systems," *J. Power Sources*, vol. 286, pp. 145–158, Jul. 2015.
[27] D. M. Weidenheimer, K. J. Donegan, and D. W. Morton, "Electronically reconfigurable battery," U.S. Patent 7 456 521 B2, 2008.
[28] P. Kumar, H. Visairo-Cruz, and S. Noble, "Reconfigurable battery pack," U.S. Patent 20 090 085 553 A1, Feb. 2009.
[29] M. D. Marr, P. G. Ross, D. E. Bryan, and S. J. McKelvie, "Reconfigurable array of backup battery units," U.S. Patent 009 910 471 B1, Jun. 2018.
[30] H. Kim and K. G. Shin, "Dynamically reconfigurable framework for a large-scale battery system," U.S. Patent 20 100 261 048 A1, 2010.
[31] T. Kim, W. Qiao, and L. Qu, "Power electronics-enabled self-X multicell batteries: A design toward smart batteries," *IEEE Trans. Power Electron.*, vol. 27, no. 11, pp. 4723–4733, Nov. 2012.
[32] Q. Ouyang, J. Chen, J. Zheng, and H. Fang, "Optimal cell-to-cell balancing topology design for serially connected lithium-ion battery packs," *IEEE Trans. Sustain. Energy*, vol. 9, no. 1, pp. 350–360, Jan. 2018.
[33] M. Mitchell, *An Introduction to Genetic Algorithms*. Cambridge, MA, USA: MIT Press, 1996.

Weiji Han (S'18) received the B.E. and first M.E. degrees from the Department of Electrical Engineering, Shandong University, China, in 2009 and 2012, respectively, and the second M.E. and the Ph.D. degrees in electrical engineering from the Department of Electrical and Computer Engineering, University of Connecticut, Storrs, CT, USA, in 2015 and 2018, respectively.

He is currently a Post-Doctoral Fellow with the Department of Electrical Engineering, Chalmers University of Technology, Gothenburg, Sweden. His research interests include modeling, analysis, and control of battery systems with applications to electric vehicles and renewable energy storage, power system, photovoltaic system, and manufacturing system.

Changfu Zou (M'16) received the B.E. degree in automotive engineering from the Beijing Institute of Technology, Beijing, China, in 2011, and the Ph.D. degree from the Department of Mechanical Engineering, University of Melbourne, Parkville, VIC, Australia, in 2017.

He was a Post-Doctoral Researcher and is currently an Assistant Professor with Automatic Control Group, Department of Electrical Engineering, Chalmers University of Technology, Gothenburg, Sweden. He was a Visiting Student Researcher with the Energy, Controls and Applications Lab, University of California, Berkeley, USA, from 2015 to 2016. His research interests include modeling and control of energy storage systems, electrified vehicles, and transport systems.

Dr. Zou was a recipient of the Excellent Graduate Award of Beijing, the Melbourne Research Scholarship, the Scholarship of National ICT Australia, and the Engineering and IT Melbourne Abroad Travel Scholarships.

Liang Zhang (S'04–M'09) received the B.E. and M.E. degrees from the Center for Intelligent and Networked Systems, Department of Automation, Tsinghua University, Beijing, China, in 2002 and 2004, respectively, and the Ph.D. degree in electrical engineering systems from the University of Michigan, Ann Arbor, MI, USA, in 2009.

He was with the Department of Industrial and Manufacturing Engineering, University of Wisconsin–Milwaukee from 2009 to 2013. He is currently an Associate Professor with the Department of Electrical and Computer Engineering, University of Connecticut, Storrs, CT, USA. His research interests include modeling, analysis, improvement, design, control, and energy-efficient operations of manufacturing and service systems, modeling and analysis of battery equalization systems, and resilient control of cyber-physical systems.

Quan Ouyang was born in Hubei, China, in 1991. He received the B.S. degree in automation from the Huazhong University of Science and Technology, China, in 2013, and the Ph.D. degree in control science and engineering from Zhejiang University, China, in 2018.

He is currently a Lecturer with the College of Automation engineering, Nanjing University of Aeronautics and Astronautics, Nanjing, China. His research interests mainly include battery management, modeling and control of fuel cell systems, and nonlinear control.

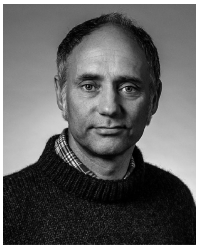

Torsten Wik received the M.Sc. degree in chemical engineering (major in applied mathematics), the Licentiate of Engineering degree in control engineering, the Ph.D. degree in environmental sciences (major in automatic control), and the Docent degree in electrical engineering from the Chalmers University of Technology, Gothenburg, Sweden, in 1994, 1996, 1999, and 2004, respectively.

From 2005 to 2007, he was a Senior Researcher with Volvo Technology, Gothenburg, researching on control system design for combustion engine test cells, and combined reformer and fuel cells. He is a Professor and the Head of the Automatic Control Group, Department of Electrical Engineering, Chalmers University of Technology. His current research interests include optimal control, model reduction, and systems with model uncertainties, with applications to energy storage, environmental, and biological systems.